SCIENCE CHINA
Chemistry

•ARTICLES•

December 2018 Vol.61 No.12: 1624–1629
https://doi.org/10.1007/s11426-018-9311-0

Controlling disorder in host lattice by hetero-valence ion doping to manipulate luminescence in spinel solid solution phosphors

Qinqin Ma[1†], Jie Wang[1†], Wei Zheng[2], Qian Wang[1], Zhiheng Li[1], Hengjiang Cong[1], Huijun Liu[3], Xueyuan Chen[2] & Quan Yuan[1*]

[1]*Key Laboratory of Analytical Chemistry for Biology and Medicine (Ministry of Education), College of Chemistry and Molecular Sciences, Wuhan University, Wuhan 430072, China;*
[2]*CAS Key Laboratory of Design and Assembly of Functional Nanostructures and Fujian Key Laboratory of Nanomaterials, Fujian Institute of Research on the Structure of Matter, Chinese Academy of Sciences, Fujian 350002, China;*
[3]*Key Laboratory of Artificial Micro- and Nano-Structures of Ministry of Education and School of Physics and Technology, Wuhan University, Wuhan 430072, China*

Received March 28, 2018; accepted June 11, 2018; published online August 16, 2018

Phosphor materials have been rapidly developed in the past decades. Developing phosphors with desired properties including strong luminescence intensity and long lifetime has attracted widespread attention. Herein, we show that hetero-valence ion doping can serve as a potent strategy to manipulate luminescence in persistent phosphors by controlling disorder in the host lattice. Specifically, spinel phosphor $Zn(Ga_{1-x}Zn_x)(Ga_{1-x}Ge_x)O_4$:Cr is developed by doping $ZnGa_2O_4$:Cr with tetravalent Ge^{4+}. Compared to the original $ZnGa_2O_4$:Cr, the doped $Zn(Ga_{1-x}Zn_x)(Ga_{1-x}Ge_x)O_4$:Cr possesses significantly enhanced persistent luminescence intensity and prolonged decay time. Rietveld refinements show that Ge^{4+} enters into octahedral sites to substitute Ga^{3+}, which leads to the co-substitution of Ga^{3+} by Zn^{2+} for charge compensation. The hetero-valence substitution of Ga^{3+} by Ge^{4+} and Zn^{2+} enriches the charged defects in $Zn(Ga_{1-x}Zn_x)(Ga_{1-x}Ge_x)O_4$:Cr, making it possible to trap large amounts of charge carriers within the defects during excitation. Electron paramagnetic resonance measurement further confirms that the amount of Cr^{3+} neighboring charged defects increases with Ge^{4+} doping. Thus charge carriers released from defects can readily combine with the neighboring Cr^{3+} to produce bright persistent luminescence after excitation ceases. The hetero-valence ion doping strategy can further be employed to develop many other phosphors and contributes to lighting, photocatalysis and bioimaging.

persistent luminescence, nanoparticle, defect, doping

Citation: Ma Q, Wang J, Zheng W, Wang Q, Li Z, Cong H, Liu H, Chen X, Yuan Q. Controlling disorder in host lattice by hetero-valence ion doping to manipulate luminescence in spinel solid solution phosphors. *Sci China Chem*, 2018, 61: 1624–1629, https://doi.org/10.1007/s11426-018-9311-0

1 Introduction

Since the discovery of Bologna stone in the 17th century, a great variety of phosphor materials have been developed [1–4], such as silicon nitride-based materials [5,6], upconversion materials [1,7–9], quantum dots [10–12], perovskites [13,14], and persistent phosphors [15–18]. The rapid development of phosphor materials has contributed to various fields including lighting, display, optoelectronic devices, photocatalysis, solar cells, biosensing and cancer therapy [19–22]. In recent years, there is a growing demand for developing phosphor materials with desired properties like high quantum yield, broad absorption band, sharp emission band, long lifetime, and good photochemical stability [23–26]. The discovery of such phosphor materials can promote

†These authors contributed equally to this work.
*Corresponding author (email: yuanquan@whu.edu.cn)

the development of advanced applications including energy saving lighting, highly efficient photocatalysis and highly sensitive biosensing [27–30].

In the past decades, several strategies have been established for developing phosphor materials, including combinatorial chemistry [31,32], cationic/anionic substitution [33,34], chemical unit cosubstitution [35], and ion doping [36–38]. Hetero-valence ion doping is an effective method to tune the luminescence properties of phosphors by doping host lattices with ions that have different valence to the substituted host ions [39]. The hetero-valence dopants usually serve as luminescent center or energy transfer meditator to influence the luminescent properties of phosphor materials [39,40]. Moreover, hetero-valence ion doping can introduce charged defects into host lattices [41–43]. The charged defects can alter the local crystal field around the activators in phosphors, leading to significant changes in the emission behaviour of the activators [44,45].

Herein, we showed that hetero-valence ion doping is a useful method to efficiently manipulate luminescence in $Zn(Ga_{1-x}Zn_x)(Ga_{1-x}Ge_x)O_4$:Cr by controlling disorder in host lattice. The developed $Zn(Ga_{1-x}Zn_x)(Ga_{1-x}Ge_x)O_4$:Cr solid-solution phosphors possess stronger persistent luminescence intensity and longer decay time compared to the undoped $ZnGa_2O_4$:Cr. Rietveld structure refinements and low temperature electron paramagnetic resonance (EPR) measurement demonstrate that a large amount of charged defects are introduced into the host lattices by hetero-valence doping of Ge^{4+}. The increased charged defects lead to considerable variation of luminescence properties. The hetero-valence ion doping strategy can open up new avenues for the exploration of phosphors with desired properties.

2 Experimental

2.1 Materials

The GeO_2 powder (99.99%) and Ga_2O_3 powder (99.99%) were purchased from Aladdin (China). The $Zn(NO_3)_2{\cdot}6H_2O$ (AR), $Cr(NO_3)_3{\cdot}9H_2O$ (AR), NaOH (AR), concentrated HNO_3 (AR) and concentrated $NH_3{\cdot}H_2O$ (28 wt%) were purchased from Sinopharm Chemical Reagent Co. (China). Deionized (DI) water (resistivity~18.25 MΩ) was used for all experiments.

2.2 Preparation of $Ga(NO_3)_3$ and Na_2GeO_3 solution

Typically, 0.01 mol of Ga_2O_3 was added into 30 mL of deionized water. Then 6 mL of concentrated nitric acid was added into the above mixture under vigorous stirring. After that, the mixture was treated at 120 °C for 8–10 h under vigorous stirring until a transparent solution was formed. The solution was transferred into a 50 mL volumetric flask and deionized water was further added to make up to volume. The concentration of the as prepared $Ga(NO_3)_3$ solution was 400 mmol/L. The Na_2GeO_3 solution was prepared as follows. Typically, 0.02 mol of GeO_2 was added into 30 mL of NaOH solution (2 mol/L). Then the mixture was left under vigorous stirring at room temperature for 6–8 h and transparent solution was formed. Afterwards, the transparent solution was transferred into a 50 mL volumetric flask and deionized water was added to make up to volume. Then Na_2GeO_3 solution (400 mmol/L) was obtained.

2.3 Preparation of $Zn(Ga_{1-x}Zn_x)(Ga_{1-x}Ge_x)O_4$:Cr

The $Zn(Ga_{1-x}Zn_x)(Ga_{1-x}Ge_x)O_4$:Cr nanoparticles were prepared by hydrothermal method. The preparation of $Zn_{1.1}Ga_{1.8}Ge_{0.1}O_4$:Cr was described as follows. Typically, $Zn(NO_3)_2$ (1.1 mmol), $Ga(NO_3)_3$ (1.8 mmol), Na_2GeO_3 (0.1 mmol) and $Cr(NO_3)_3$ (0.0075 mmol) were added into deionized water (12 mL) under vigorous stirring. Concentrated ammonium hydroxide was dropwise added into the above solution until the pH of the reaction system reaches 8.5. Then, the solution was stirred for 1 h at room temperature and was further transferred into an autoclave for hydrothermal treatment at 220 °C for 6 h. The as-prepared $Zn_{1.1}Ga_{1.8}Ge_{0.1}O_4$:Cr nanoparticles were collected by centrifugation. The $ZnGa_2O_4$:Cr nanoparticles were synthesized with $Zn(NO_3)_2$ (1 mmol), $Ga(NO_3)_3$ (2 mmol) and $Cr(NO_3)_3$ (0.0075 mmol) with the similar protocol. The $Zn_{1.2}Ga_{1.6}Ge_{0.2}O_4$:Cr nanoparticles were also synthesized with $Zn(NO_3)_2$ (1.2 mmol), $Ga(NO_3)_3$ (1.6 mmol), Na_2GeO_3 (0.2 mmol) and $Cr(NO_3)_3$ (0.0075 mmol) by the above described method.

2.4 Measuring the persistent luminescence decay of $Zn(Ga_{1-x}Zn_x)(Ga_{1-x}Ge_x)O_4$:Cr colloidal solution

Briefly, 1 mL of $ZnGa_2O_4$:Cr colloidal dispersion (1 mg/mL) and $Zn_{1.1}Ga_{1.8}Ge_{0.1}O_4$:Cr colloidal solution (1 mg/mL) were added into a 48-well-plate, respectively. The plate was put into a living image IVIS® spectrum and an orange LED (1000 lumen) was used to illuminate the plate for 2 min. After that, the LED excitation was removed and the decay images were recorded. The decay images were captured at 1, 3, 5, 7 and 10 min, respectively. The decay images of the second and the third activation were recorded with the same manner.

3 Results and discussion

3.1 Characterization of $Zn(Ga_{1-x}Zn_x)(Ga_{1-x}Ge_x)O_4$:Cr

A series of $Zn(Ga_{1-x}Zn_x)(Ga_{1-x}Ge_x)O_4$:Cr nanoparticles were perpared through doping different amounts of Ge^{4+} into $ZnGa_2O_4$:Cr with a simple hydrothermal approach. The

shape and crystal structure of $Zn(Ga_{1-x}Zn_x)(Ga_{1-x}Ge_x)O_4$:Cr nanoparticles were characterized with transmission electron microscopy (TEM) and X-ray powder diffraction (XRD) measurement. As shown in Figure 1(a–c), $ZnGa_2O_4$:Cr, $Zn_{1.1}Ga_{1.8}Ge_{0.1}O_4$:Cr and $Zn_{1.2}Ga_{1.6}Ge_{0.2}O_4$:Cr are all well-dispersed with uniform shape. The XRD patterns of the $Zn(Ga_{1-x}Zn_x)(Ga_{1-x}Ge_x)O_4$:Cr nanoparticles can be indexed to cubic spinel phase of $ZnGa_2O_4$, indicating the formation of a homogeneous spinel solid solution (Figure S2, Supporting Information online) [16,46]. The luminescent properties of $Zn(Ga_{1-x}Zn_x)(Ga_{1-x}Ge_x)O_4$:Cr nanoparticles were further systematically investigated. The photoluminescence spectra (Figure 1(d)) show that the phosphors exhibit broad emission in the range of 650–750 nm. The peak at around 715 nm is the Stokes phonon sideband line (S-PSB), which is indexed to Cr^{3+} ions occupying the ideal octahedral sites [47]. Another peak at about 696 nm is the N2 zero phonon line indexed to Cr^{3+} ions in octahedral sites that are distorted by neighbouring charged defects [47]. Notably, the S-PSB line becomes weaker whereas the N2 line grows stronger with the increase of doped Ge^{4+}, suggesting that hetero-valence doping of Ge^{4+} modifies the local structure of Cr^{3+}. As N2 is the dominate emission line responsible for persistent luminescence in $ZnGa_2O_4$:Cr [47], the increase of N2 line may lead to considerable changes in the persistent luminescence of $Zn(Ga_{1-x}Zn_x)(Ga_{1-x}Ge_x)O_4$:Cr. The persistent luminescence decay curves of the $Zn(Ga_{1-x}Zn_x)(Ga_{1-x}Ge_x)O_4$:Cr nanoparticles are systematically measured and are shown in Figure 1(e). The doped phosphors possess significantly enhanced persistent luminescence intensity compared to the undoped $ZnGa_2O_4$:Cr. Also, the persistent luminescence intensity increases with increasing the amount of doped Ge^{4+}. Notably, the persistent luminescence intensity in $Zn_{1.1}Ga_{1.8}Ge_{0.1}O_4$:Cr and $Zn_{1.2}Ga_{1.6}Ge_{0.2}O_4$:Cr at 10 min of decay is 2.8 and 8.0 times of that in $ZnGa_2O_4$:Cr, respectively. The luminescence decay images of $ZnGa_2O_4$:Cr and $Zn_{1.1}Ga_{1.8}Ge_{0.1}O_4$:Cr after excitation ceases were further measured. As shown in Figure 1(f), the $Zn_{1.1}Ga_{1.8}Ge_{0.1}O_4$:Cr is much brighter than $ZnGa_2O_4$:Cr and the decay time of $Zn_{1.1}Ga_{1.8}Ge_{0.1}O_4$:Cr is also much longer than that of $ZnGa_2O_4$:Cr. After the excitation ceases, the persistent luminescence of $ZnGa_2O_4$:Cr colloidal solution almost disappears at 10 min of decay, whereas the $Zn_{1.1}Ga_{1.8}Ge_{0.1}O_4$:Cr colloidal solution still displays obvious persistent luminescence. Moreover, the two phosphors can be readily reactivated with a commercially avaliable orange LED. Similar brighter persistent luminescence and longer decay time in $Zn_{1.1}Ga_{1.8}Ge_{0.1}O_4$:Cr are observed. The luminescence intensity of the decay images is further quantified and shown in Table 1. The persistent luminescence intensity in $Zn_{1.1}Ga_{1.8}Ge_{0.1}O_4$:Cr is about 2 times of that in $ZnGa_2O_4$:Cr. The above results thus clearly suggest that hetero-valence ion doping can effectively modify the luminescent properties of $Zn(Ga_{1-x}Zn_x)(Ga_{1-x}Ge_x)O_4$:Cr.

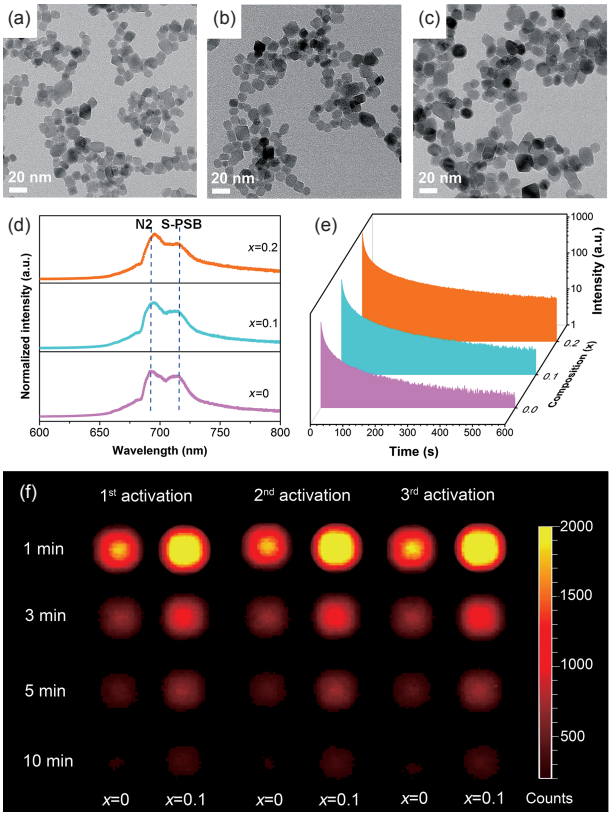

Figure 1 (a) TEM images of $ZnGa_2O_4$:Cr, (b) $Zn_{1.1}Ga_{1.8}Ge_{0.1}O_4$:Cr and (c) $Zn_{1.2}Ga_{1.6}Ge_{0.2}O_4$:Cr nanoparticles. (d) Photoluminescence spectra of $Zn(Ga_{1-x}Zn_x)(Ga_{1-x}Ge_x)O_4$:Cr nanoparticles. N2: N2 zero photon line. S-PSB: Stokes phonon sideband line. (e) Luminescence decay curves in $Zn(Ga_{1-x}Zn_x)(Ga_{1-x}Ge_x)O_4$:Cr nanoparticles. (f) Luminescence decay images of $ZnGa_2O_4$:Cr and $Zn_{1.1}Ga_{1.8}Ge_{0.1}O_4$:Cr colloid dispersion (1 mg/mL) after excitation with a LED (color online).

3.2 Rietveld refinement crystal structure of $Zn(Ga_{1-x}Zn_x)(Ga_{1-x}Ge_x)O_4$:Cr

According to previous studies, charged defects play a vital role in the generation of persistent luminescence [17,27,48]. Charged defects can store excitation energy and then gradually release the energy to activators to produce persistent luminescence after excitation ceases [17,27,48]. Before studying the charged defects in the $Zn(Ga_{1-x}Zn_x)(Ga_{1-x}Ge_x)O_4$:Cr, the structures variation of the $Zn(Ga_{1-x}Zn_x)(Ga_{1-x}Ge_x)O_4$:Cr induced by hetero-valence ion doping was investigated. Rietveld refinements were performed to investigate the crystal structures of $Zn(Ga_{1-x}Zn_x)(Ga_{1-x}Ge_x)O_4$:Cr [49]. The atomic position in $Zn(Ga_{1-x}Zn_x)(Ga_{1-x}Ge_x)O_4$:Cr were systematically determined. The result of Rietveld refinement for $ZnGa_2O_4$:Cr is shown in Figure 2(a), and the corresponding crystal structure of $ZnGa_2O_4$:Cr is illustrated in Figure 2(b). In $ZnGa_2O_4$:Cr, Zn^{2+} ions occupy the tetrahedral sites and Ga^{3+} ions occupy the octahedral sites. Also, $ZnGa_2O_4$:Cr exhibits a slight inversion [50]. That is, a small amount of Zn^{2+} ions is in octahedral coordination and the

Table 1 The luminescence intensity of decay images of $ZnGa_2O_4$:Cr and $Zn_{1.1}Ga_{1.8}Ge_{0.1}O_4$:Cr colloid dispersion shown in Figure 1(f)

	1st activation (10^4)		2nd activation (10^4)		3rd activation (10^4)	
	x=0	x=0.1	x=0	x=0.1	x=0	x=0.1
1 min	29.8	50.9	31.3	53.7	34.5	60.3
3 min	12.6	20.6	12.5	21.5	13.1	22.5
5 min	7.92	12.6	8.29	13.8	8.38	14.3
10 min	4.01	6.63	4.05	6.67	4.07	6.90

same amount of Ga^{3+} ions is in tetrahedral coordination. These charged antisite defects play a crucial role in the generation of persistent luminescence in $ZnGa_2O_4$:Cr [47,48]. Figure 2(c) shows the Rietveld refinement of $Zn_{1.1}Ga_{1.8}Ge_{0.1}O_4$:Cr. In $Zn_{1.1}Ga_{1.8}Ge_{0.1}O_4$:Cr, the doped Ge^{4+} ions enter into the octahedral sites (Figure 2(d)). Compared with $ZnGa_2O_4$:Cr, more Ga^{3+} ions occupy the tetrahedral sites and more Zn^{2+} ions occupy the octahedral sites in $Zn_{1.1}Ga_{1.8}Ge_{0.1}O_4$:Cr. The Rietveld refinement of $Zn_{1.2}Ga_{1.6}Ge_{0.2}O_4$:Cr is shown in Figure 2(e). In $Zn_{1.2}Ga_{1.6}Ge_{0.2}O_4$:Cr, the doped Ge^{4+} ions are all located in octahedral sites (Figure 2(f)). Impressively, the amounts of Ga^{3+} ions at tetrahedral sites and Zn^{2+} ions at octahedral sites in $Zn_{1.2}Ga_{1.6}Ge_{0.2}O_4$:Cr are much higher than that in $Zn_{1.1}Ga_{1.8}Ge_{0.1}O_4$:Cr. These crystal structures clearly suggest that the amount of antisite defects in $Zn(Ga_{1-x}Zn_x)(Ga_{1-x}Ge_x)O_4$:Cr increases with raising the amount of doped Ge^{4+}. Moreover, the atomic positions of $Zn(Ga_{1-x}Zn_x)(Ga_{1-x}Ge_x)O_4$:Cr nanoparticles (Table S1, Supporting Information online) show that the substitution of Ga^{3+} ions by Ge^{4+} ions at the octahedral sites leads to the co-substitutio of Ga^{3+} ions by Zn^{2+} ions, which can be ascribed to the charge compensation effect. These above results thus clearly suggest that hetero-valence ion doping can change the atomic position in $Zn(Ga_{1-x}Zn_x)(Ga_{1-x}Ge_x)O_4$:Cr, and the variation of atomic position further introduces charged defects into host lattices.

3.3 Charged defects in $Zn(Ga_{1-x}Zn_x)(Ga_{1-x}Ge_x)O_4$:Cr

The charged defects in $Zn(Ga_{1-x}Zn_x)(Ga_{1-x}Ge_x)O_4$:Cr nano-

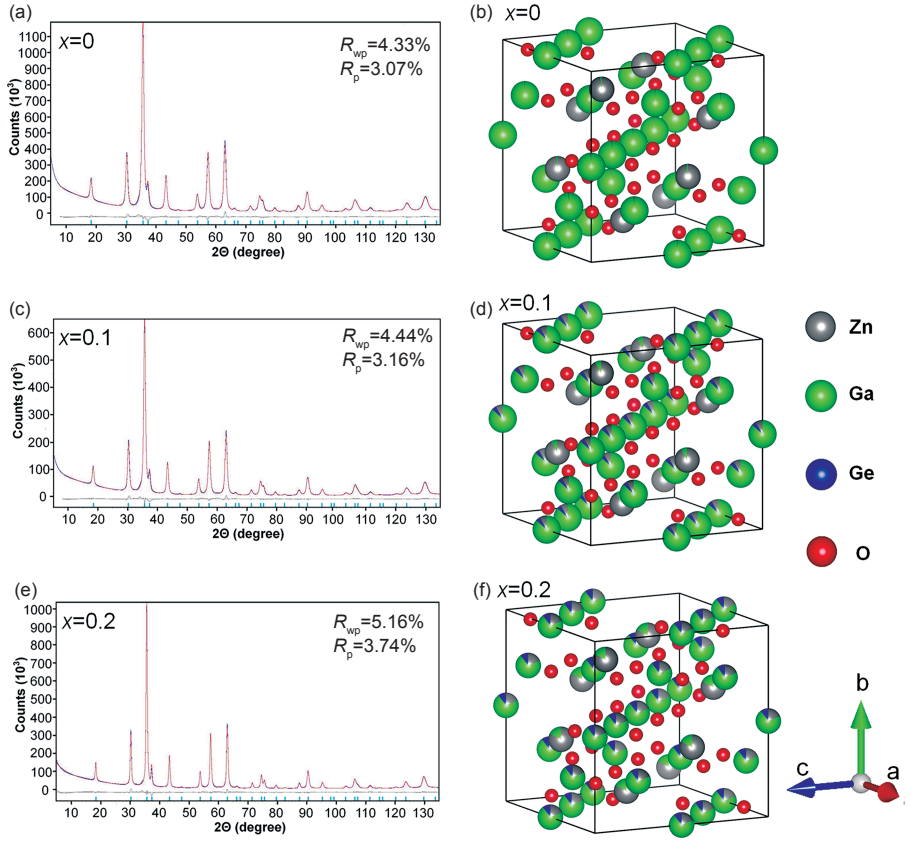

Figure 2 (a) Rietveld refinement of $ZnGa_2O_4$:Cr. (b) Schematic illustration of $ZnGa_2O_4$:Cr unit cell. (c) Rietveld refinement of $Zn_{1.1}Ga_{1.8}Ge_{0.1}O_4$:Cr. (d) Schematic illustration of $Zn_{1.1}Ga_{1.8}Ge_{0.1}O_4$:Cr unit cell. (e) Rietveld refinement of $Zn_{1.2}Ga_{1.6}Ge_{0.2}O_4$:Cr. (f) Schematic illustration of $Zn_{1.2}Ga_{1.6}Ge_{0.2}O_4$:Cr unit cell (color online).

particles were further determined based on the above structural refinement results. The amounts of positively charged defects Ge°_{Ga}, Ga°_{Zn}, and negatively charged defects Zn'_{Ga} in host lattices were determined. As shown in Table 2, the content of charged defects in $ZnGa_2O_4$:Cr is about 6%, in good agreement with previous studies [47]. The amount of charged defects in the doped $Zn(Ga_{1-x}Zn_x)(Ga_{1-x}Ge_x)O_4$:Cr is significantly increased with increasing the amount of doped Ge^{4+}. Compared to $ZnGa_2O_4$:Cr, the amounts of charged defects in $Zn_{1.1}Ga_{1.8}Ge_{0.1}O_4$:Cr and $Zn_{1.2}Ga_{1.6}Ge_{0.2}O_4$:Cr are increased by about 5.0 and 12.7 times, respectively. The above results clearly show that large amounts of charged defects have been introduced into $Zn(Ga_{1-x}Zn_x)(Ga_{1-x}Ge_x)O_4$:Cr by hetero-valence ion doping.

3.4 Electron paramagnetic resonance measurements

As mentioned above, the charged defects can alter the local structure of neighboring activators. Low temperature electron paramagnetic resonance (EPR) measurements were further performed to investigate the amount of Cr^{3+} neighboring charged defects in $Zn(Ga_{1-x}Zn_x)(Ga_{1-x}Ge_x)O_4$:Cr. The EPR spectra of the perturbed Cr^{3+} neighboring charged defects and the unperturbed Cr^{3+} in ideal octahedral sites were also simulated, respectively. As shown in Figure 3(a), the band at around 1320 G (red shadow) is indexed to the absorption of perturbed Cr^{3+} and the band at around 1720 G (blue shadow) is assigned to the absorption of unperturbed Cr^{3+}. In $ZnGa_2O_4$:Cr, the absorption band of perturbed Cr^{3+} is weaker than that of the unperturbed Cr^{3+}, indicating that a small amount of perturbed Cr^{3+} exit in the crystal. Whereas in the doped $Zn(Ga_{1-x}Zn_x)(Ga_{1-x}Ge_x)O_4$:Cr, the absorption band of perturbed Cr^{3+} gradually grows stronger and the absorption band of unperturbed Cr^{3+} becomes weaker with the increase of doped Ge^{4+}. These results suggest that the content of perturbed Cr^{3+} in $Zn(Ga_{1-x}Zn_x)(Ga_{1-x}Ge_x)O_4$:Cr significantly increases with hetero-valence Ge^{4+} doping, which can be ascribed to the increased charged defects in host lattice. The mechanism of charged defects increasing in $Zn(Ga_{1-x}Zn_x)(Ga_{1-x}Ge_x)O_4$:Cr induced by hetero-valence ion doping is further illustrated in Figure 3(b). The hetero-valence substitution of Ga^{3+} by Ge^{4+} leads to a significant increase of inversion and the co-substitution of Ga^{3+} by Zn^{2+} in the nanocrystals. The significant changes of the cationic

Table 2 Charged defects in $Zn(Ga_{1-x}Zn_x)(Ga_{1-x}Ge_x)O_4$:Cr. Ge°_{Ga}:Ge^{4+} ion in the octahedral site. Zn'_{Ga}:Zn^{2+} ion in the octahedral site. Ga°_{Zn}:Ga^{3+} ion in the tetrahedral site. The negative and positive charges are represented by dash and dot respectively

Composition (x)	Ge°_{Ga}	Zn'_{Ga}	Ga°_{Zn}
0	0	0.03	0.03
0.1	0.1	0.18	0.08
0.2	0.2	0.38	0.18

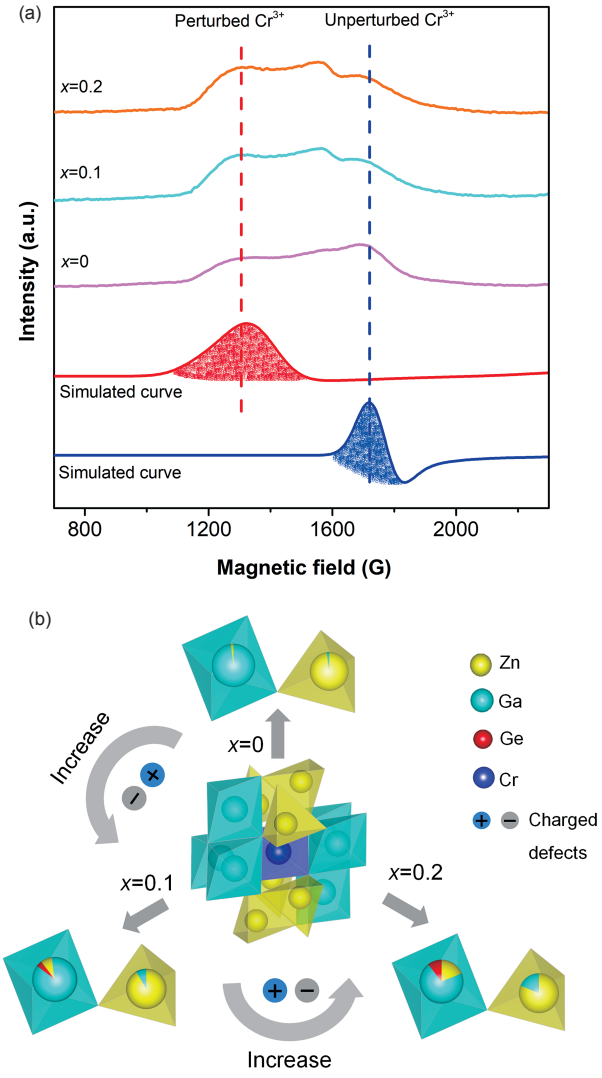

Figure 3 (a) EPR spectra of $Zn(Ga_{1-x}Zn_x)(Ga_{1-x}Ge_x)O_4$:Cr. (b) Schematic illustration of charged defects increasing in $Zn(Ga_{1-x}Zn_x)(Ga_{1-x}Ge_x)O_4$:Cr induced by hetero-valence ion doping (color online).

occupation introduce a large amount of charged defects in $Zn(Ga_{1-x}Zn_x)(Ga_{1-x}Ge_x)O_4$:Cr. Under excitation, the charged defects in host lattice can store excitation energy. After excitation ceases, the energy is gradually released from the charged defects and the neighboring perturbed Cr^{3+} ions can receive the released energy to generate persistent luminescence [47,48]. To conclude, the increased charged defects can modify the local structure of neighboring activators, leading to changes in luminescent properties of $Zn(Ga_{1-x}Zn_x)(Ga_{1-x}Ge_x)O_4$:Cr.

4 Conclusions

In this article, we have highlighted that hetero-valence ion doping can serve as a potent strategy to introduce charged defects in persistent phosphors for manipulating the lumi-

nescent properties. The persistent luminescence intensity in $Zn(Ga_{1-x}Zn_x)(Ga_{1-x}Ge_x)O_4$:Cr is enhanced and the decay time is prolonged compared with the undoped $ZnGa_2O_4$:Cr. The Ge^{4+} ions doping efficiently introduces charged defects in $Zn(Ga_{1-x}Zn_x)(Ga_{1-x}Ge_x)O_4$:Cr, leading to the increase of Cr^{3+} neighboring charged defects. As a result, the energy released from the charged defects can be efficiently transferred to the neighboring Cr^{3+} to produce bright persistent luminescence after excitation ceases. This study can open exciting new possibilities for the exploration of phosphor materials with desired properties, and it can further contribute to a wide range of applications like lighting, photocatalysis and bioimaging.

Acknowledgements This work was supported by the National Key R&D Program of China (2017YFA0208000), the National Natural Science Foundation of China (21675120, 21325104), and the CAS/SAFEA International Partnership Program for Creative Research Teams. We sincerely thank Prof. Zhenxing Wang from Huazhong University of Science and Technology for his assistance in EPR simulation. The EPR simulation is conducted with the SPIN developed by Andrew Ozarowski in the National High Magnetic Field Laboratory, USA.

Conflict of interest The authors declare that they have no conflict of interest.

Supporting information The supporting information is available online at http://chem.scichina.com and http://link.springer.com/journal/11426. The supporting materials are published as submitted, without typesetting or editing. The responsibility for scientific accuracy and content remains entirely with the authors.

1 Zhu X, Su Q, Feng W, Li F. *Chem Soc Rev*, 2017, 46: 1025–1039
2 Wu BY, Wang HF, Chen JT, Yan XP. *J Am Chem Soc*, 2011, 133: 686–688
3 Maldiney T, Bessière A, Seguin J, Teston E, Sharma SK, Viana B, Bos AJJ, Dorenbos P, Bessodes M, Gourier D, Scherman D, Richard C. *Nat Mater*, 2014, 13: 418–426
4 Wang W, Cheng Z, Yang P, Hou Z, Li C, Li G, Dai Y, Lin J. *Adv Funct Mater*, 2011, 21: 456–463
5 Bielec P, Schnick W. *Angew Chem Int Ed*, 2017, 56: 4810–4813
6 Lin CC, Tsai YT, Johnston HE, Fang MH, Yu F, Zhou W, Whitfield P, Li Y, Wang J, Liu RS, Attfield JP. *J Am Chem Soc*, 2017, 139: 11766–11770
7 Zhou J, Liu Q, Feng W, Sun Y, Li F. *Chem Rev*, 2015, 115: 395–465
8 Dong H, Sun LD, Wang YF, Ke J, Si R, Xiao JW, Lyu GM, Shi S, Yan CH. *J Am Chem Soc*, 2015, 137: 6569–6576
9 Huang L, Zhao Y, Zhang H, Huang K, Yang J, Han G. *Angew Chem Int Ed*, 2017, 56: 14400–14404
10 Michalet X, Pinaud FF, Bentolila LA, Tsay JM, Doose S, Li JJ, Sundaresan G, Wu AM, Gambhir SS, Weiss S. *Science*, 2005, 307: 538–544
11 Wu P, Yan XP. *Chem Soc Rev*, 2013, 42: 5489–5521
12 Xu G, Zeng S, Zhang B, Swihart MT, Yong KT, Prasad PN. *Chem Rev*, 2016, 116: 12234–12327
13 Wei Y, Deng X, Xie Z, Cai X, Liang S, Ma P, Hou Z, Cheng Z, Lin J. *Adv Funct Mater*, 2017, 27: 1703535
14 Zou S, Liu Y, Li J, Liu C, Feng R, Jiang F, Li Y, Song J, Zeng H, Hong M, Chen X. *J Am Chem Soc*, 2017, 139: 11443–11450
15 Wu SQ, Yang CX, Yan XP. *Adv Funct Mater*, 2017, 27: 1604992
16 Li Z, Zhang Y, Wu X, Huang L, Li D, Fan W, Han G. *J Am Chem Soc*, 2015, 137: 5304–5307
17 Huang B. *Inorg Chem*, 2015, 54: 11423–11440
18 Huang B, Sun M. *Phys Chem Chem Phys*, 2017, 19: 9457–9469
19 Li Z, Zhang Y, Wu X, Wu X, Maudgal R, Zhang H, Han G. *Adv Sci*, 2015, 2: 1500001
20 Song L, Li PP, Yang W, Lin XH, Liang H, Chen XF, Liu G, Li J, Yang HH. *Adv Funct Mater*, 2018, 28: 1707496
21 Zhou Z, Zheng W, Kong J, Liu Y, Huang P, Zhou S, Chen Z, Shi J, Chen X. *Nanoscale*, 2017, 9: 6846–6853
22 Wang J, Ma Q, Hu XX, Liu H, Zheng W, Chen X, Yuan Q, Tan W. *ACS Nano*, 2017, 11: 8010–8017
23 Song L, Lin XH, Song XR, Chen S, Chen XF, Li J, Yang HH. *Nanoscale*, 2017, 9: 2718–2722
24 Gai S, Li C, Yang P, Lin J. *Chem Rev*, 2014, 114: 2343–2389
25 Qin X, Liu X, Huang W, Bettinelli M, Liu X. *Chem Rev*, 2017, 117: 4488–4527
26 Lécuyer T, Teston E, Ramirez-Garcia G, Maldiney T, Viana B, Seguin J, Mignet N, Scherman D, Richard C. *Theranostics*, 2016, 6: 2488–2523
27 Wang J, Ma Q, Wang Y, Shen H, Yuan Q. *Nanoscale*, 2017, 9: 6204–6218
28 Xia Z, Ma C, Molokeev MS, Liu Q, Rickert K, Poeppelmeier KR. *J Am Chem Soc*, 2015, 137: 12494–12497
29 Punjabi A, Wu X, Tokatli-Apollon A, El-Rifai M, Lee H, Zhang Y, Wang C, Liu Z, Chan EM, Duan C, Han G. *ACS Nano*, 2014, 8: 10621–10630
30 Shang M, Li C, Lin J. *Chem Soc Rev*, 2014, 43: 1372–1386
31 Danielson E, Devenney M, Giaquinta DM, Golden JH, Haushalter RC, McFarland EW, Poojary DM, Reaves CM, Weinberg WH, Wu XD. *Science*, 1998, 279: 837–839
32 Park WB, Singh SP, Sohn KS. *J Am Chem Soc*, 2014, 136: 2363–2373
33 Han S, Qin X, An Z, Zhu Y, Liang L, Han Y, Huang W, Liu X. *Nat Commun*, 2016, 7: 13059
34 Tsai YT, Chiang CY, Zhou W, Lee JF, Sheu HS, Liu RS. *J Am Chem Soc*, 2015, 137: 8936–8939
35 De Trizio L, Manna L. *Chem Rev*, 2016, 116: 10852–10887
36 Chen D, Wang Y. *Nanoscale*, 2013, 5: 4621–4637
37 Dong H, Sun LD, Feng W, Gu Y, Li F, Yan CH. *ACS Nano*, 2017, 11: 3289–3297
38 Huang B, Peng D, Pan C. *Phys Chem Chem Phys*, 2017, 19: 1190–1208
39 Deng R, Qin F, Chen R, Huang W, Hong M, Liu X. *Nat Nanotech*, 2015, 10: 237–242
40 Shen S, Wang Q. *Chem Mater*, 2013, 25: 1166–1178
41 Liu Y, Zhang X, Hao Z, Wang X, Zhang J. *Chem Commun*, 2011, 47: 10677–10679
42 He H, Zhang Y, Pan Q, Wu G, Dong G, Qiu J. *J Mater Chem C*, 2015, 3: 5419–5429
43 Liu J, Lian H, Shi C. *Opt Mater*, 2007, 29: 1591–1594
44 Zheng W, Zhou S, Chen Z, Hu P, Liu Y, Tu D, Zhu H, Li R, Huang M, Chen X. *Angew Chem Int Ed*, 2013, 52: 6671–6676
45 Dou Q, Zhang Y. *Langmuir*, 2011, 27: 13236–13241
46 Abdukayum A, Chen JT, Zhao Q, Yan XP. *J Am Chem Soc*, 2013, 135: 14125–14133
47 Gourier D, Bessière A, Sharma SK, Binet L, Viana B, Basavaraju N, Priolkar KR. *J Phys Chem Solids*, 2014, 75: 826–837
48 Huang B. *Phys Chem Chem Phys*, 2016, 18: 25946–25974
49 Manual U, TOPAS V. *General Profile and Structure Analysis Software for Powder Diffraction Data*. Karlsruhe:, 2000
50 Hill RJ, Craig JR, Gibbs GV. *Phys Chem Miner*, 1979, 4: 317–339